



Virtual anthropology: Forensic applications to cranial skeletal remains from the Spanish Civil War



Laia Sevillano Oriola^{a,b}, Núria Armentano Oller^{a,c}, Neus Martínez-Abadías^{b,*}

^a Departament de Biologia Animal, de Biologia Vegetal i d'Ecologia (BABVE), Universitat Autònoma de Barcelona, Edifici C., 08193 Bellaterra, Spain

^b Departament de Biologia Evolutiva, Ecologia i Ciències Ambientals (BEECA), Facultat de Biologia, Universitat de Barcelona (UB), Av. Diagonal, 643. Planta 2, 08028 Barcelona, Spain

^c Laboratori de Paleopatologia, Museu d'Arqueologia de Catalunya, Passeig de Santa Madrona, 39, 08038 Barcelona, Spain

ARTICLE INFO

Article history:

Received 17 June 2022

Received in revised form 14 October 2022

Accepted 19 October 2022

Available online 21 October 2022

Keywords:

Virtual anthropology

3D reconstruction

Photogrammetry

Craniofacial morphology

Spanish Civil War

ABSTRACT

Biological and forensic anthropologists face limitations while studying skeletal remains altered by taphonomic alterations and perimortem trauma, such as in remains from the Spanish Civil War. However, virtual anthropology techniques can optimize the information inferred from fragmented and deformed remains by generating and restoring three-dimensional bone models. We applied a low-cost 3D modelling methodology based on photogrammetry to develop novel forensic applications of virtual 3D skull reconstruction, assembly, restoration and ancestry estimation. Crania and mandible fragments from five Spanish Civil War victims were reconstructed with high accuracy, and only one cranium could not be assembled due to extensive bone loss. Virtual mirroring successfully restored reconstructed crania, producing 3D models with reduced deformation and perimortem trauma. High correlation between traditional and virtual craniofacial measurements confirmed that 3D models are suitable for forensic applications. Craniometric databases of world-wide and Spanish populations were used to assess the potential of discriminant analysis to estimate population ancestry. Our protocol correctly estimated the continental origin of 86.7 % of 15 crania of known origin, and despite low morphological differentiation within European populations, correctly identified 54.5 % as Spanish and 27.3 % of them with high posterior probabilities. Two restored crania from the Civil War were estimated as Spanish, and one as a non-Spanish European. Results were not conclusive for one cranium and did not confirm previous archeological hypotheses. Overall, our research shows the potential to assess the presence of foreign volunteers in the Spanish Civil War and highlights the added value of 3D-virtual techniques in forensic anthropology.

© 2022 The Authors. Published by Elsevier B.V. This is an open access article under the CC BY-NC-ND license (<http://creativecommons.org/licenses/by-nc-nd/4.0/>).

1. Introduction

Skeletal remains are the most commonly used remnants to infer the life history of past people. Since the origins of human osteology and biological anthropology research, experts have analyzed human skeletal remains to infer biological data such as sex [1], age [2,3], and height [4]. Bones can also inform about health and lifestyle factors like diet, physical activity, and well-being, so that researchers can identify pathologies and injuries that people suffered during their life and caused their death [5]. This information is of invaluable importance in scenarios of catastrophes and war crimes.

The Spanish Civil War (1936–1939) and posterior dictatorship (1939–1975) caused thousands of civilian deaths, including the Spanish population involved in this conflict, but also volunteers from

other European countries that served in the “International Brigade” [6]. The Spanish Government approved by law the opening and body exhumation of mass graves from the Spanish Civil War in 2007 [7], and by 2015 almost 2000 individuals had been exhumed. However, only 18% of the victims have been identified anthropologically or genetically [8]. One of the main obstacles for individual identification is the disappearance over time of antemortem data and the increasing lack of living direct descendants from the Spanish Civil War victims, which limits the accuracy of the genetic identifications [9,10].

Skeletal remains can also be used for individual identification [11]. However, the method is less reliable than the genetic identification and can be more challenging, especially when bone morphology is altered by perimortem trauma and taphonomic postmortem modifications that compromise the recognition of characteristic traits of individuals when they were alive [5]. Perimortem trauma, such as gunshots, are commonly found in war

* Corresponding author.

E-mail address: neusmartinez@ub.edu (N. Martínez-Abadías).

victims and typically damage the bone creating comminuted, radiating fractures, as well as bone fragmentation and plastic deformation [5,12–15]. Taphonomic modifications produced after burial and embedding by biological and geological factors such as dehydration, scavengers, ground, or ice pressure can also cause bone breakage and deformation [5,16–18].

The loss of bone original state and morphology hinders the process of anthropometric and biological profiling of the skeletal remains, compromising future identifications of the individual's body. The conventional and widely accepted routine for forensic and biological anthropologists specialized in analyzing highly fragmented and deformed skeletal remains consists in gluing bone fragments in anatomical concordance [19,20]. This is a laborious practice that requires extensive practice and expertise. Some bone fragments can be very small or too fragile to handle, whereas others may not be preserved, making this task even more challenging. Although deformations can alter the original dimensions, standard measurements are usually taken on the reconstructed crania and mandibles using spreading and sliding calipers and a mandibulometer to characterize the craniofacial morphology of the individuals [5].

Virtual anthropology can be used to complement and optimize the manual processes of skull reconstruction and measurement [21–23]. Several imaging techniques, such as computed tomography (CT) [24], laser scanning [25] and structured light scanning (SLS) [26], have been used since the early 1990 s by forensic scientists and paleoanthropologists to produce high-quality 3D models of bones [24]. These techniques entail a whole new level of possibilities in the anthropological field. Bone digitalization allows permanent availability and easy access to virtual 3D models of skeletal remains, higher reproducibility of results, fast data exchange, and can be used to develop forensic applications [26,27].

The reconstruction and restoration of skeletal fragments is one of the main forensic applications of virtual anthropology. This process can be achieved using techniques that include computer-assisted manual assembly of fragments, virtual replacement of specific bone structures from complete specimens, and virtual reconstruction by mirroring structures [26,28]. From the reconstructed 3D models, advanced quantitative shape analysis encompassing geometric morphometric methods [28] can be used to assess the anatomy of bones, and to compare the morphology with other individuals, populations and species [24,29,30]. Virtual anthropology has already been successfully applied to assess bone injuries and trauma [22,23], as well as to estimate parameters for the biological profile such as sex [31,32] and age-at-death [32,33].

Ancestry identification is another useful forensic application that can be applied to virtually reconstructed crania [34,35]. In anthropological sciences, human crania are the most widely analyzed bones, as their complex morphology and extended variation can be associated to sexual, age and population variation [36–39]. Moreover, craniofacial traits present moderate to high heritability [40,41] and craniofacial morphological variation can be used as a proxy for genetic variation [38,39,42]. Current forensic methods to estimate population ancestry are mainly based on craniometric data [43–45] and use Howells' world-wide craniometric database [46] for their ancestry estimations, although some methods combine craniofacial and dental morphological data [47]. Increasingly over the years, novel approaches based on geometric morphometrics are being developed for ancestry estimation [31,48].

Although its increasing popularity, virtual anthropology is not yet a widely spread practice among biological anthropologists working with archaeological human remains. The main disadvantage of 3D modelling is the elevated cost of the scanning and associated software for image processing [25]. Additional disadvantages involve the requirement of specialized personnel for scanning, and the difficulty to transport the scanning equipment, such as computed tomography

scanners, to the archaeological fields. Photogrammetry is a more affordable and convenient option for 3D scanning skeletal remains [49]. This technique consists of processing overlapping 2D digital photographs of a single structure from multi-angle, convergent perspectives to create a 3D model with accurate position, shape, and size reconstructions [50,51]. The basic requirement for photogrammetric scanning is a digital single-lens reflex camera (DLRS) and specialized software, like Agisoft Metashape [52] or other freely available software [53].

In this study, we applied virtual 3D methodologies based on photogrammetric techniques to reconstruct, assemble and restore fragmented skull remains from the Spanish Civil War. We assessed whether this virtual method can improve existing limitations in manual reconstruction of skulls affected by taphonomic postmortem modifications and perimortem trauma fracturing the bone in few fragments. Moreover, we used craniometric measurements taken on restored crania to extend the biological profiling of the skeletal remains and to test hypotheses about their population ancestry.

2. Materials and methods

2.1. Sample of skeletal remains from the Spanish Civil War

The sample consists of crania and mandibles from five Spanish Civil War non-identified victims located in Catalonia, a Northeastern region in Spain, during the Catalan Government mass grave project 2017–2018. Remains were exhumed from two different locations. Individuals 1 and 2 (INDIV1 and INDIV2) were found in El Cogul (Lleida), whereas the rest of individuals (INDIV3, INDIV4 and INDIV5) were exhumed from two different graves in Barcelona. The discovery of the remains was unintentional in all cases during forest and construction works. All the remains were in provisional deposit at the Universitat Autònoma de Barcelona for anthropological study, including the biological profiling and pathological analysis.

INDIV1 involves the cranial remains from a young male individual, with estimated age between 25 and 30 years old, including an entire and well-preserved cranium, and a fragmented mandible (Fig. 1a) [54]. The cranium presents an entrance bullet hole of 9 mm of diameter in the right mastoid region, where an irradiate perimortem fracture originates and pierces the right temporal, sphenoid, and frontal bones. The bullet was found inside the cranium with no outlet hole. The left zygomatic bone is fractured and the zygomatic arch is missing. The mandible is separated in a larger fragment including the mandibular body and right ramus, and a smaller fragment corresponding to the left ramus, with bone loss between mandibular fragments.

INDIV2 consisted in the cranial remains from a male individual, with estimated age between 40 and 50 years old, including craniofacial and mandible fragments (Fig. 1b) [54]. The cranium is broken in three pieces with perimortem features along the edges. The largest and most complete piece covers the splanchnocranium and neurocranium, in which the frontal bone is fractured by an irregular horizontal fracture with perimortem alterations, the left temporo-parietal region is fragmented, and the cranial base is lost. The other two fragments include the occipital and the maxillary bones. No evidence of bullet impact was found due to cranial bone loss. The mandible is also fragmented in three parts, including the mandibular body and two smaller fragments of the right and left mandibular ramus. Both craniofacial and mandibular fragments present taphonomic alterations, including greenish coloration due to metal oxidation and orange incrustations caused by iron oxidation.

INDIV3 included the cranial remains from a male individual, with estimated age between 30 and 39 years old, including an entire and well-preserved and robust cranium and a fragmented mandible (Fig. 1c) [55]. Two perimortem orifices are found in the cranium: the entrance bullet hole of 8.8 mm of diameter in the right temporo-

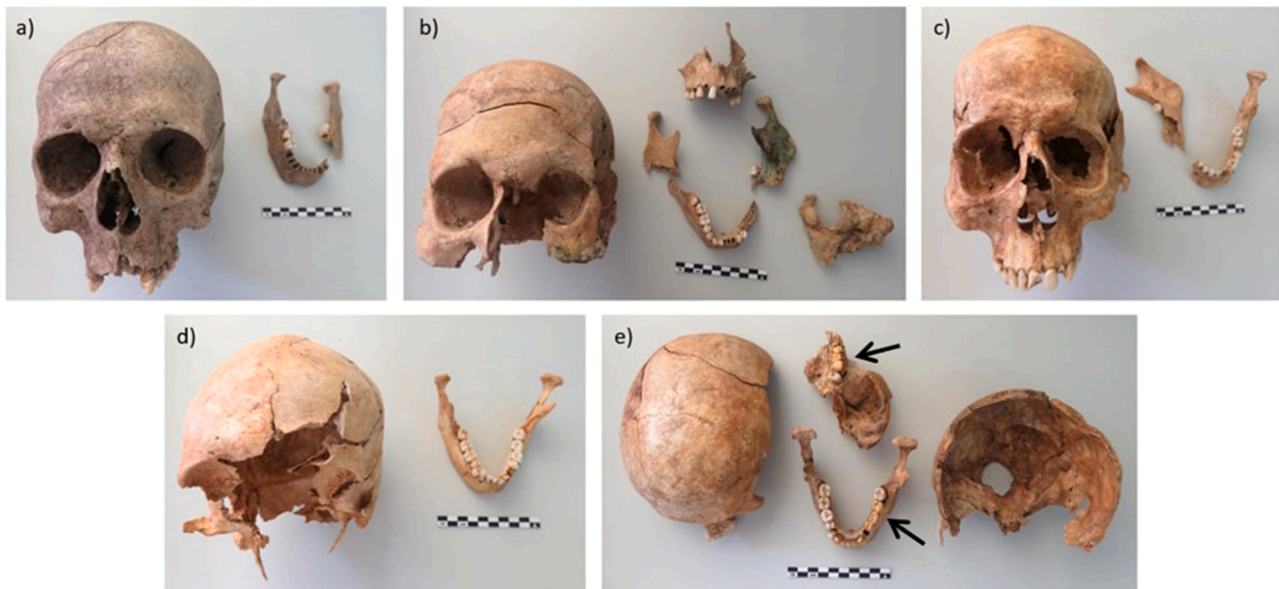


Fig. 1. Cranial and mandible remains of Spanish Civil War victims. a) INDIV1; b) INDIV2; c) INDIV3; d) INDIV4; e) INDIV5. Arrows highlight the gold dental caps visible in the left mandible and maxilla of INDIV5.

parietal region and the outlet hole of 16 mm of diameter in the left temporo-parietal region. These injuries present associated irradiated fractures, which cross the right parietal bone transversely, the left temporal bone transversely and the orbits. Plastic deformation is found, as well as diastasis of right and left temporal squama, right sphenoidal wing, and temporo-parieto-occipital suture. The mandible is fragmented in a larger fragment including almost the whole mandibular body and the left ramus, and a smaller fragment of the right ramus and body.

INDIV4 involved the cranial remains from a male individual, with estimated age between 30 and 39 years old, including a poorly preserved cranial fragment and a well-preserved mandible (Fig. 1d) [55]. The cranium presents comminuted fractures, whereas most of the splanchnocranium and cranial base are lacking. Cranial deformation is visible due to an irradiated fracture crossing the cranial vault, taphonomic fractures and transverse squashing in the neurocranium. Presence of perimortem irradiated fractures suggest a bullet wound, although no orifices are found due to bone loss. The mandible presents evidence of a bullet entrance orifice of 9 mm of diameter in the left sigmoid notch.

INDIV5 is represented by the cranial remains from a robust male individual, with estimated age between 30 and 35 years old, including a fragmented cranium and a well-preserved mandible (Fig. 1e) [55]. The cranial remains include three fragments: the base of the cranium, the calotte, and the left maxilla. Three different bullet orifices associated to irradiated fractures are found in the cranium: an oval-shaped entrance of 11.5 mm of maximum diameter in the right posterior parietal bone, a second entrance orifice of 9 mm of diameter in the left temporal bone, and its outlet orifice of 8.6 mm of diameter in the right parietal. A comminuted fracture is also found in the splanchnocranium, causing bone loss and plastic deformation, as well as diastasis of both temporal squama and parieto-occipital suture. The mandible is not fragmented, however there is a visible bullet orifice of 9.5 mm of diameter in the left mandibular angle and associated irradiated fractures.

Previous forensic analysis hypothesized on the basis of anthropometric traits and associated objects that the remains of individuals INDIV3 and INDIV5 could belong to European non-Spanish individuals that participated in the Spanish Civil War at the "International Brigade" [55]. These individuals presented a skeletal height and robustness that was above the average in the Spanish

population and wore gold dental caps and rings that were unusual in Spain at that time. In this study, we tested this hypothesis by assessing the population ancestry of the skeletal remains.

2.2. Photogrammetry: reconstruction of 3D models

To generate 3D models of skulls or bone fragments we used a Nikon D3300 DLRS digital camera mounted on a tripod and connected to a Foldio360 turntable from Orangemonkie®. Each fragment was held on a circular support and placed on the turntable. While turning 360°, a total of 36 photos were taken every 10°. After a complete turn, the camera angle was changed twice (Fig. 2). Afterwards, the skull or bone fragment was changed into a perpendicular position and another round of pictures was taken. A minimum of 4 sets of photographs were taken to completely capture the 3D shape of the bone from all possible angles and positions. A scale bar was placed on the turntable for a minimum of 2 sets of photographs. The Agisoft Metashape v1.6.5 software [52] was used to align photographs, build dense clouds, and generate 3D models with texture. The scaling was done in the Metashape Professional software scaling mode, which transforms pixels into millimeters when selecting two points of known distance, in this case two points of the reconstructed scale bar.

2.3. Virtual assembly of 3D bone fragments

Virtual assembly of cranial or mandibular fragments was performed using Amira 2019.2 software (Mercury Computer Systems, Inc. Chelmsford, MA). To accurately join the fragments in a three-dimensional space, the 3D models representing adjacent fragments were thoroughly evaluated to locate a minimum of five pairs of common anatomical points along the fissures of each fragment in at least two different planes. *Landmark 2-sets* option in Amira was used to register the 3D cartesian coordinates of the corresponding points. The two sets of landmark coordinates were then matched by performing a rigid transformation between the 3D models that virtually joined the bone fragments. Using this procedure, the cranium and mandible of each individual was also articulated by recording the 3D coordinates of anatomical corresponding points located on the mandibular condyle and temporal mandibular fossa, as well as on tooth wear facets when possible.

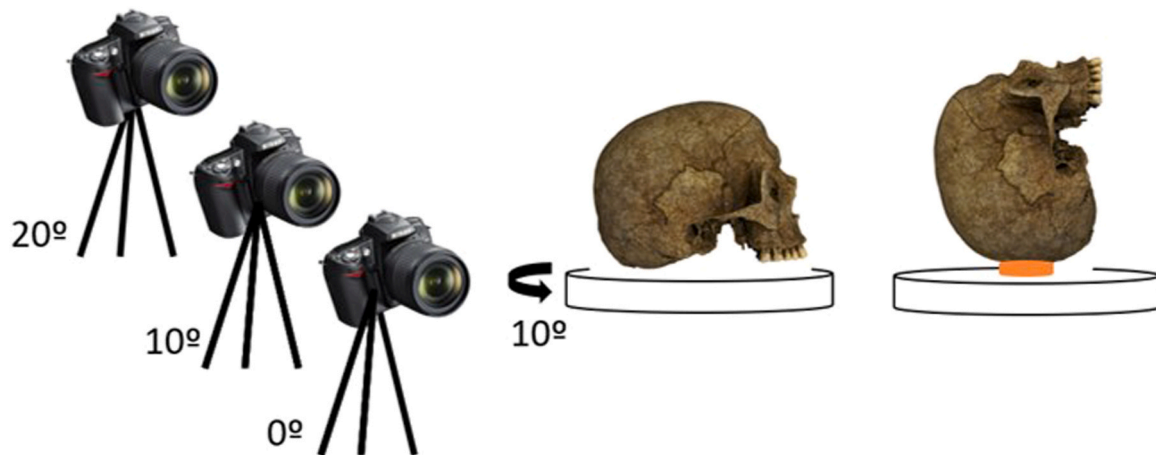


Fig. 2. Camera mounted on tripod and cranium positioning on turntable for generating 3D photogrammetry models.

2.4. Cranial restoration by mirroring

Virtual restoration was performed in Amira 2019.2 by mirroring the less deformed or damaged half of each cranium. After morphological assessment, the more deformed half was manually removed and the selected half was duplicated, inverted, and joined to the other half using the Amira *Landmark 2-sets* function. A minimum of 9 landmarks of anatomical concordance between both halves were registered for accurate 3D matching. For qualitative comparison of the original and mirrored models, a superimposition of both meshes, applying rigid transformation and scaling, was performed.

2.5. Traditional and virtual craniometry

Cranial and mandibular metric measurements were taken on manually reconstructed dry bones following the traditional methodology in biological anthropology, using spreading and sliding calipers and a mandibulometer [37,56,57] (Supplementary table 1). In those cases in which bone fragments could not be correctly glued together, it was not possible to measure all dimensions on dry bones with the traditional method.

For virtual craniometry, the 3D cartesian coordinates of a set of 63 anatomical landmarks [5,46,56,58,59] were registered over the reconstructed cranium and mandible using the open-source software 3DSlicer [60] (Supplementary table 2). Linear measurements were calculated as Euclidean distances between the 3D coordinates of the two landmarks defining the origin and end of each skull measurement. The mandibular angle was calculated as the inverse cosine between the vector defined by the inferior border of the mandibular body and the vector defined by the posterior border of the mandibular ramus. Mandibular length was calculated as the linear distance between Gnathion and a median point between the right and left Gonions.

Each skull was measured three times using both the traditional and virtual methods, and mean values were used for subsequent analyses. Intra-observer error for each method was assessed using the Technical Error Measurement (TEM), a measure of error produced when a single object is measured different times [61]. TEM is expressed in the same measurement units and is calculated with the following formula,

$$TEM = \sqrt{\frac{\sum_{i=1}^n (x_{1i} - x_{2i})^2}{2n}}$$

where x is a pair of measurements taken at different times, and n is the total number of measurements. Considering an acceptable measurement range error for anthropologists of 2 mm [62], TEM

values below 2 mm were considered negligible. Precision in landmark acquisition was assessed as the variation in landmark placement. The average Standard Deviation (SD) for each landmark coordinate was calculated [63] and SD values below 0.5 mm were considered as highly precise, values between 0.5 mm and 1 mm were considered as precise, and values greater than 1 mm were considered as not precise.

The agreement between traditional and virtual methodologies was evaluated by a correlation analysis between the measurements obtained from both techniques on each skull. Normality was assessed with a Shapiro-Wilk test and non-parametric variables were tested using Spearman correlation. Bland-Altman plots were produced in R v4.1 [64] using the *BlandAltmanLeh* package [65] as a graphical and statistical tool for method comparison [66].

2.6. Ancestry estimation

A reference craniometric database was assembled pooling data from previously published databases. This included a cranial sample of 54 Spanish males retrieved from the Olóriz collection [67,68], as well as 1309 world-wide male cranial sample retrieved from the Howells collection [46] (Data publicly available at <http://volweb.utk.edu/~auerbach/HOWL.htm>) (Fig. 3). These cranial collections are widespread used databases in anthropological research [69–71].

We selected 18 craniometric measures that were common in the Olóriz and Howells databases (Supplementary table 3). Variables with more than 50 % of missing values were excluded from the analysis and missing values in the Olóriz database were substituted with the variable mean value. To measure these craniometric distances in the skulls from the Spanish Civil War, we measured the restored models.

We performed a Principal Component Analysis (PCA) based on craniometric measures to explore craniofacial variation among world-wide populations, by grouping samples according to their continental origin, and among European populations. We also performed a Canonical Variates Analysis (CVA) to identify the craniofacial traits that maximized the separation between populations. PCA and CVA were performed and plotted using PAST v4.03 [72].

To assess ancestry estimation, we implemented two sets of Linear Discriminant Analysis (LDA) and discriminant functions in R v4.1 [64] using the *MASS* package [73]. The first set of discriminant functions included world-wide populations and was used to assess European ancestry. The second set of discriminant functions, which only included European populations (Spanish, Berg, Norse and Zavalár), was used to obtain a more precise assessment of the European origin of each cranium. Posterior probabilities were calculated



Fig. 3. Populations extracted from Howells (red) and Olóriz (blue) cranial collections. Craniometric data of male individuals was extracted from the following populations: 1 - Mokapu (n = 51); 2 - Santa Cruz (n = 51); 3 - Arikara (n = 42); 4 - Easter Island (n = 49); 5 - Peru (n = 55); 6 - Eskimo (n = 53); 7 - Norse (n = 55); 8 - Berg (n = 56); 9 - Zalavár (n = 53); 10 - Spanish (n = 54); 11 - Dogon (n = 47); 12 - Teita (n = 33); 13 - Bushman (n = 41); 14 - Zulu (n = 55); 15 - Andaman (n = 35); 16 - Hainan (n = 45); 17 - Atayal (n = 29); 18 - Phillipi (n = 50); 19 - Anyang (n = 42); 20 - Ainu (n = 48); 21 - Northern Japan (n = 55); 22 - Southern Japan (n = 50); 23 - Guam (n = 30); 24 - Tolai (n = 56); 25 - Australi (n = 52); 26 - Tasmania (n = 45); 27 - Northern Maori (n = 10); 28 - Moriori (n = 57); 29 - Southern Maori (n = 10).

for unknown-ancestry crania using the *lda.predict* command in the MASS package.

The accuracy of ancestry prediction of this set of discriminant functions were tested on a sample of 15 crania of known origin. Most crania were retrieved from the collection of the Universitat de Barcelona (find Table 1 in the results section), which comprised 10 crania of individuals excavated from medieval Spanish sites, and four crania from non-Spanish populations, including one crania of an individual from a Guanche population in Canary Islands, one crania of an individual from a Saharawi population in Northwest Africa, one individual from Equatorial Guinea, and one individual from Philippines. Finally, we also retrieved data from a Spanish Civil War victim exhumed from the town of Gurb (Table 1) that was identified as Spanish [74].

The ancestry of each Spanish Civil War crania was tested individually using the reference craniometric database. Since reconstructed crania were fragmented and all measurements could not be taken even in the mirrored restored crania, we adjusted the number of craniometric variables used for the ancestry estimation to the measurements available in each cranium. New discriminant functions were re-calculated in each case, and the accuracy of ancestry prediction was tested with known Spanish crania.

3. Results

3.1. Photogrammetry

Three-dimensional models were successfully created following the photogrammetry workflow. Overall, high mesh quality was

Table 1

Ancestry predictions in crania of known origin. Continental and European predictions associated to posterior probabilities are provided. UB: non-identified crania retrieved from the collection of Universitat de Barcelona. Known origin based on the geographical origin of the site in which the remains were exhumed. GURB: cranium of an identified victim of the Spanish Civil War. * Incorrect classifications.

Individual cranium	Known origin	Continent prediction	Posterior probability	European prediction	Posterior probability
UB.1	Guanche	Africa	0.61	-	
UB.2	Saharawi	Africa	0.85	-	
UB.3	Eq. Guinea	Africa	0.85	-	
UB.4	Philippines	Asia	0.60	-	
UB.5	Spanish	Europe	0.69	Spanish	0.45
UB.6	Spanish	Europe	0.70	Spanish	0.55
UB.7	Spanish	Europe	0.87	Spanish	0.56
UB.8	Spanish	Europe	0.99	Spanish	0.99
UB.9	Spanish	Europe	0.99	Zalavár*	0.45
UB.10	Spanish	Europe	0.92	Norse*	0.39
UB.11	Spanish	Europe	0.81	Norse*	0.51
UB.12	Spanish	Europe	0.97	Norse*	0.72
UB.13	Spanish	Asia*	0.41	Spanish	0.95
UB.14	Spanish	Asia*	0.53	Zalavár*	0.56
GURB	Spanish	Europe	0.98	Spanish	0.99

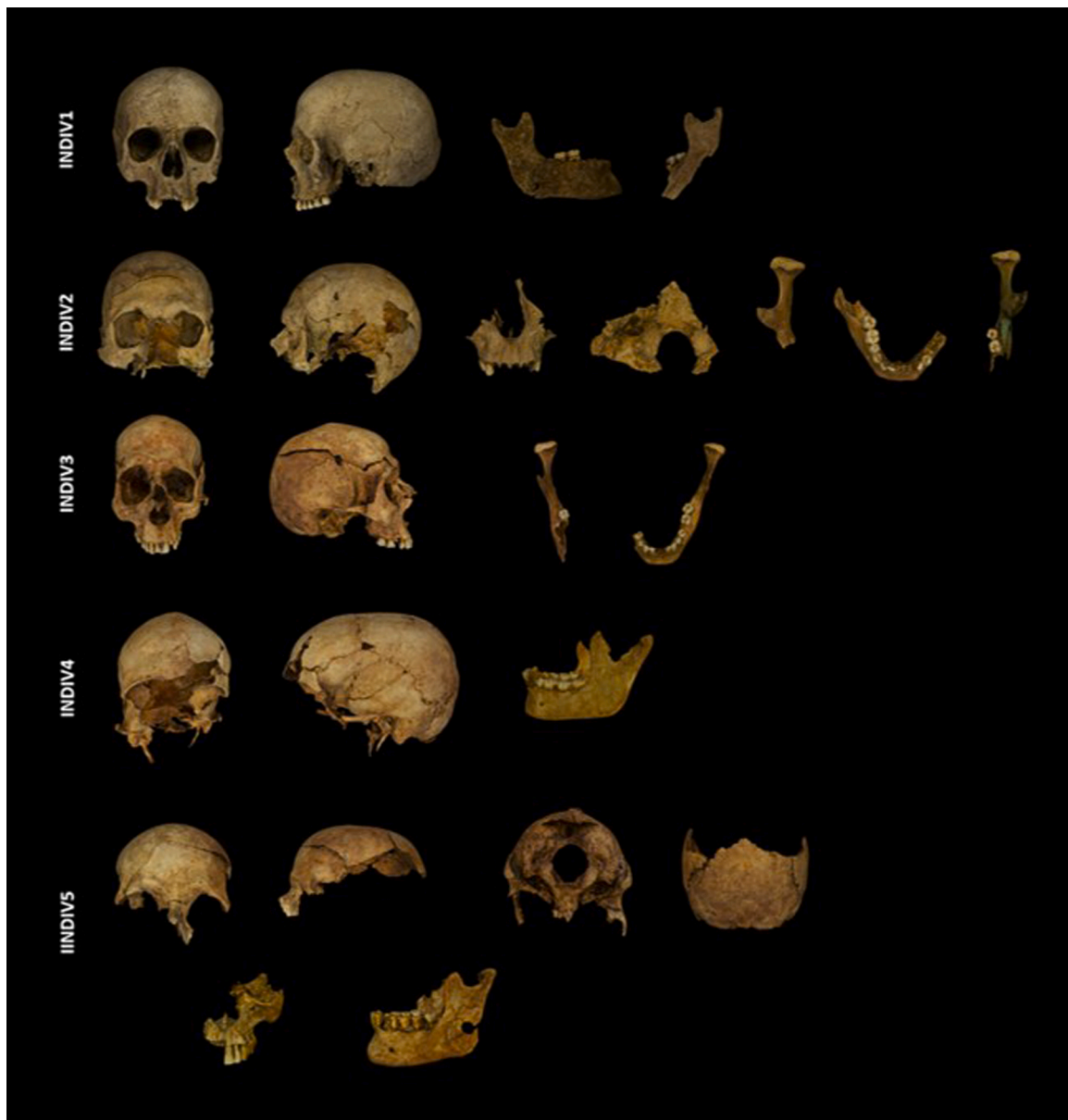


Fig. 4. Photogrammetry-based three-dimensional models of cranial and mandibular skeletal remains of five victims of the Spanish Civil War. 3D models not to scale.

achieved for all fragments (Fig. 4, Supplementary Figs. 1–5), even the smallest ones, with only small reconstruction defects that did not significantly affect bone anatomy and could be fixed with post-processing. Perimortem trauma, like fractures and projectile wounds, were reconstructed with highest accuracy. Texture accuracy was also achieved, remarkably reflecting taphonomic coloration and other materials like gold dental caps (Fig. 4, INDIV5 mandible).

3.2. Virtual reconstruction and assembly of 3D skull fragments

Virtual assembly of 3D fragments was successful for four out of five individuals, either using the anatomic correspondence between fragments along concordant fractures, or the assembly of the temporo-mandibular articulation (Fig. 5, Supplementary Figs. 6–9). Only the cranium and mandible of INDIV4 were not correctly assembled due to the severe cranial taphonomic deformation and bone loss, which included bilateral temporal's mandibular fossa.

Despite the high fragility and incompleteness of the remains, facial restoration by virtual assembly was achieved even in INDIV2

and INDIV5, in which manual assembly by gluing the bone fragments was not feasible. Mandibular fragments of INDIV1 presented fractures without anatomical concordance due to bone loss, however their temporo-mandibular assembly allowed both 3D fragments to be anatomically placed.

3.3. Virtual restoration by mirroring

Craniofacial restoration by mirroring one half of the cranium was achieved in four out of five individuals. The right half of INDIV1 cranium was mirrored and as a result it was possible to restore the left zygomatic arch that was originally lost (Fig. 6, Supplementary Fig. 10).

In INDIV2, the right half was mirrored, resulting in an almost complete recovery of the right temporal, parietal, and zygomatic bones, as well as a decrease in deformation (Fig. 6, Supplementary Fig. 11).

In INDIV3, the right half was mirrored, resulting in a more accurate cranial reconstruction, in which facial and frontotemporal

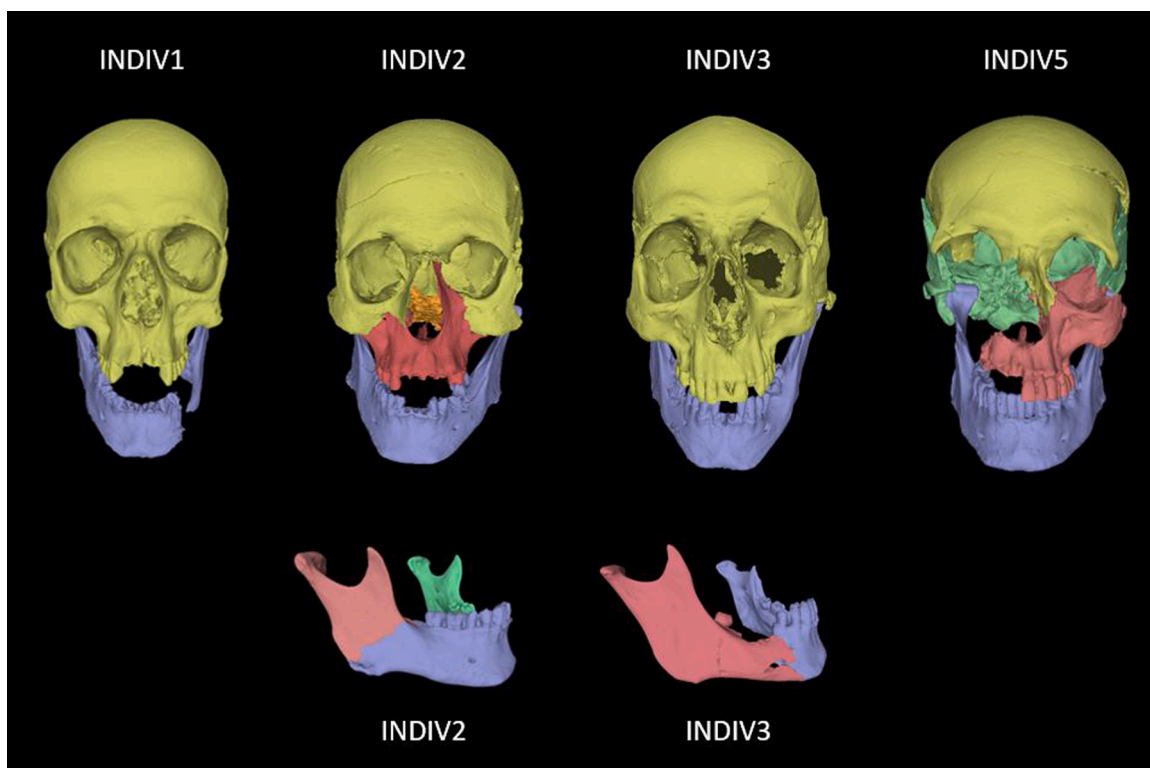


Fig. 5. Virtual assembly and articulation of cranial and mandible remains.

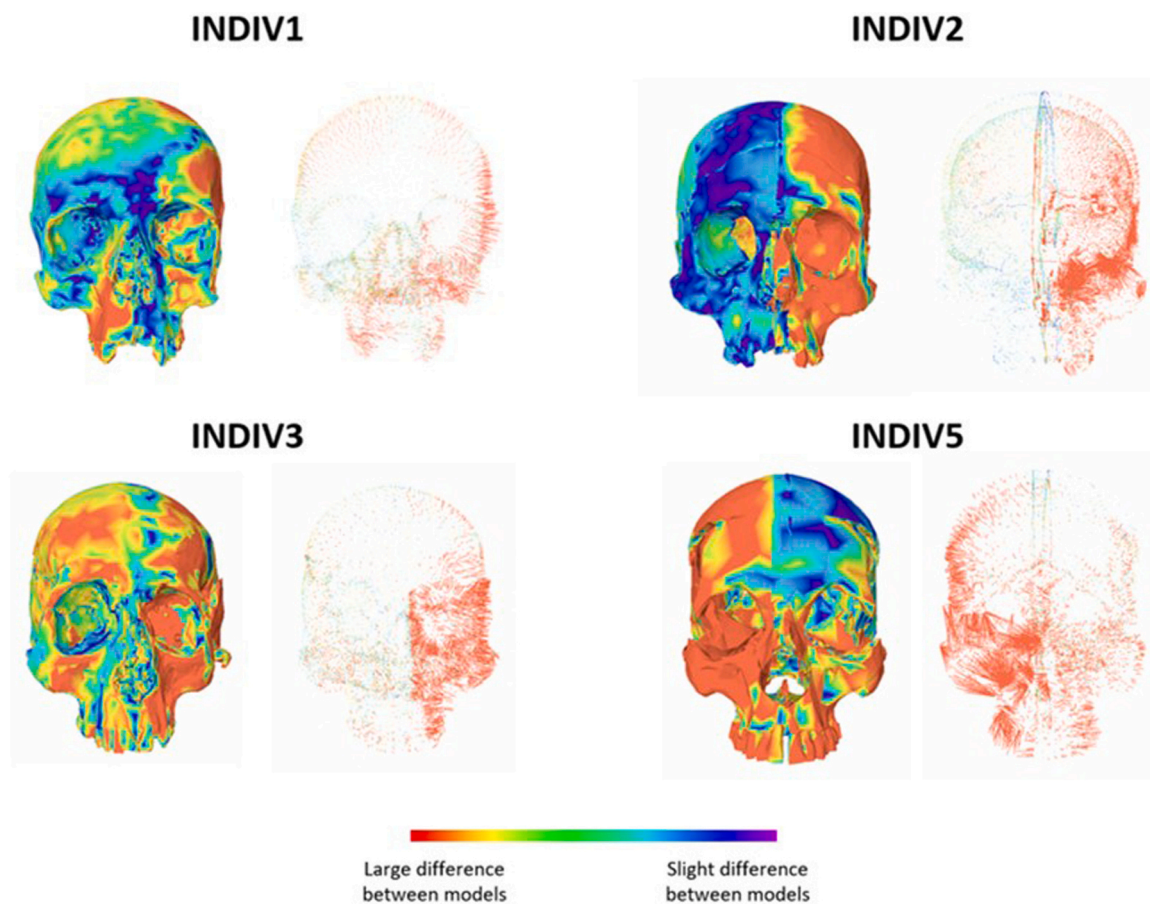


Fig. 6. Virtually restored model by mirroring technique and original mesh superimposition. Original and mirrored 3D meshes were compared by superimposition and differences were shown as heatmaps and vector maps, with red areas indicating where the largest differences occur.

deformations were almost completely restored (Fig. 6, Supplementary Fig. 12). There was originally a bullet outlet hole in the left temporal bone that was replaced by the entrance hole present in the right temporal bone. Since the deformation associated to this perimortem injury was less severe, the right half of the skull was chosen to mirror the cranium of INDIV3. However, the irradiated fracture associated to the entrance hole was duplicated, resulting in a reduction of maximum cranial breadth. For this reason, this measurement was discarded when we assessed the ancestry estimation of this individual in the subsequent forensic applications.

In INDIV5, the left half was mirrored and as a result the right maxilla, zygomatic and frontotemporal bones were almost completely reconstructed (Fig. 6, Supplementary Fig. 13). A downside of this reconstruction was the reproduction of a horizontal fracture in the right parietal bone, which introduced slight deformation in the right cranial vault visible in the mediolateral axis. Therefore, maximum cranial breadth and biauricular breadth were excluded in forensic applications assessing this individual.

3.4. Virtual and traditional craniometry

Comparison of virtual and traditional craniometric measurements showed an acceptable intra-observer error for both techniques, with Technical Error Measurement (TEM) values usually inferior to 1.5 mm (traditional TEM range: 0.99–3.02 mm; virtual TEM range: 0.64–0.8 mm). The only exception showing high error (TEM=3.02) was detected in the traditional measurements of INDIV5. When measured using the virtual technique, the skull of this individual presented a significantly lower intra-observer error (TEM=0.8 mm), showing a better performance of virtual craniometry. Overall, the three-dimensional landmarks were positioned with high precision, with 81 % of landmarks presenting SD values below 0.5 mm.

Virtual and traditional measurements were highly correlated (Spearman's $\rho > 0.99$; $p < 0.001$), despite few exceptions. The measurement with the highest percentage error in all individuals was mandibular length, with differences ranging between 15 % and 25 %, indicating that the proposed estimation for mandibular length was not accurate. Bland-Altman plots further assessing virtual and traditional measurements in each individual (Fig. 7) showed that the mean of differences between virtual and traditional measurements ranged between 0 and 1 mm, except for INDIV4, in which the mean difference between virtual and traditional measurements was close to 2 mm, probably due to a less precise scaling of the virtual model. Bland-Altman plots also showed a proportional bias in the measurements. While short measurements (<100 mm) showed a tendency to present values below the mean line and around 0, long measurements (>100 mm) presented values above the mean line and greater dispersion. This indicated that shorter measures showed higher agreement between virtual and traditional techniques, while differences of 3 or 4 millimeters could be found in longer measurements. Overall, the comparison between traditional and virtual measurements confirmed that virtual models generated and scaled by photogrammetry are adequate for forensic applications.

3.5. Ancestry estimation

Populations from the five world continents showed high variability in cranial morphology, and their 95 % confidence ellipses largely overlapped in the morphospace generated by a PCA (Fig. 8a). Likewise, European populations showed a general overlap in the PCA plot, except for the Spanish population, which showed an increased range of variation along PC1 (Fig. 8b). In both PCAs, PC1 was associated with size differences: individuals with larger dimensions displayed positive PC1 scores, whereas individuals with smaller dimensions displayed negative scores.

Canonical variate analysis maximized differences between groups, allowing a relative discrimination between continental populations (Fig. 9a). CV1 separated individuals with longer more projected facial morphologies on the right, from shorter and retracted faces on the left (Fig. 9a). Within European populations, the CVA revealed that despite relative overlap in the range of morphological variation between Berg, Spanish, Zalavár and Norse populations, there is potential in craniofacial morphology to predict population ancestry from crania of unknown origin that display morphologies that fall outside the common range of variation (Fig. 9b). CV1 separated dolichocephalic crania with narrow noses on the right from brachycephalic crania with wider nasal morphology on the left (Fig. 9b). Zalavár and Norse completely overlapped on the CVA (Fig. 9b), showing that it could not be possible to differentiate between individuals from these populations.

Discriminant functions were calculated using Linear Discriminant Analysis on the continental and European reference samples. The predictive power of both databases was tested using 15 crania of known origin (Table 1). Within the continental database, 13 out of 15 crania (86.7 %) were correctly classified, with an associated posterior probability that ranged from 0.60 to 0.99. Incorrectly classified crania (13.3 %) were associated to posterior probabilities of 0.41 and 0.53 (Table 1). Therefore, a minimum posterior probability threshold value of 0.6 for continental prediction was assumed in subsequent analyses.

The European database was tested with 11 crania of known Spanish origin. Six crania (54.5 %) were estimated as Spanish, with a posterior probability range of 0.45–0.99 (Table 1). Three crania (27.3 %) were incorrectly classified as Norse (posterior probability range of 0.39–0.72), and two (18.2 %) as Zalavár (posterior probabilities of 0.45 and 0.56). As the highest probability of an incorrect classification was 0.72, the threshold for correct classifications was set to 0.73. With this criterion, only 3 out of 11 crania (27.3 %) were correctly classified with high posterior probability.

Ancestry predictions for crania of victims of the Spanish Civil War are provided in Table 2. Results showed that INDIV1 was classified as European with 0.96 posterior probability, and as Norse within European populations with 0.74 posterior probability (Table 2), discarding the initial hypothesis of Spanish ancestry. INDIV2 was classified as European with 0.56 posterior probability, and as Spanish with 0.86 posterior probability. Considering that this posterior probability was higher than the threshold, the initial hypothesis of Spanish ancestry was accepted. INDIV3 was classified as Asian with 0.77 posterior probability, and Spanish ancestry with 0.95 posterior probability, and thus the hypothesis of non-Spanish European ancestry was not accepted. Finally, INDIV5 was classified as African with 0.53 posterior probability, and Spanish ancestry with 0.52 posterior probability. These results were not conclusive and therefore, the hypothesis of a non-Spanish European ancestry could not be either accepted or rejected.

4. Discussion

Three-dimensional models generated using our photogrammetry protocol were reconstructed with high quality standards, comparable to previous studies [51]. The resulting virtual models were valuable input data for further forensic applications, especially in the case of fragile skeletal remains. We managed to reconstruct, assemble, and restore the craniofacial remains of four out of five victims from the Spanish Civil War (Fig. 4). Virtual reconstruction and assembly enabled us to join bone fragments and to measure craniometric dimensions that could not be performed on dry bones by traditional reconstruction methods. Finally, we gathered continental and European reference craniometric databases and used craniometric traits measured on restored crania 3D models to test

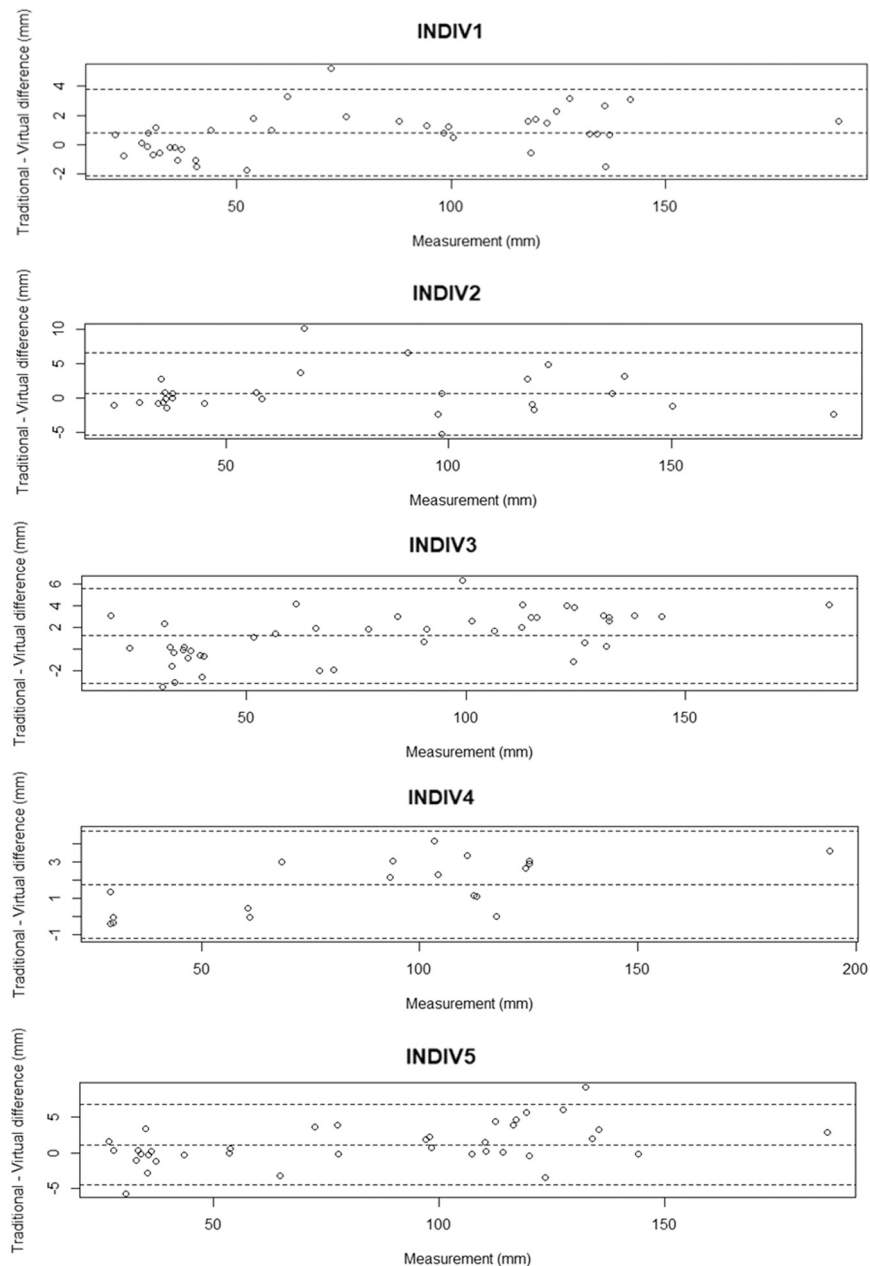


Fig. 7. Bland-Altman plots comparing traditional and virtual craniometric methods. The X axis represents the skull measurement in mm, whereas the Y axis indicates the difference in mm of each pair of traditional and virtual measurements. The central dotted line indicates the mean value of the differences between both measurement techniques, and the upper and lower lines indicate the limits of agreement (mean \pm 1.96SD). Except for mandibular length, all measurements taken with both traditional and virtual techniques were included in the Bland-Altman analyses.

hypotheses about the population ancestry of the Spanish Civil War victims.

Our optimized photogrammetry protocol generated 3D models with a fast acquisition process of approximately 15 min. However, the generation of a mesh with highest quality was a computationally demanding process that increased the processing time from an average of 2–3 h to more than 10 h, depending on the computer power. Similar processing times have been reported by other photogrammetry studies [75–77]. Our scanning protocol generated 3D models of either complete or fragmented crania and mandibles (Fig. 4), with the smallest fragment being a mandibular condyle of 9 cm. Our virtual assembly protocol (Fig. 5) concluded in a full reconstruction of the two individuals with fragmented skulls (INDIV2 and INDIV5), and a correct mandible-cranium articulation in most cases, even in an individual with incomplete mandible (INDIV1).

Since anatomic correspondence between fragments is required for correct assembly, our method only failed to join fragments caused by damages that involved major bone loss (INDIV4).

Overall, our results suggest that despite virtual reconstruction and assembly require extensive expertise and long processing times [78], virtual methods can be successfully applied in complete and partially fragmented skulls. The main advantage of virtual anthropology is that 3D models can be easily accessed, exchanged and virtually manipulated without the risk of damaging the remains [26,27]. Moreover, in cases where manual reconstruction is not feasible because bones are too fragile to handle or cranial fragments are deformed and cannot be physically fit together, virtual methods can represent an added value. Current limitations of virtual methods mainly involve the reconstruction and assembly of small bone fragments. According to previous studies, accurate 3D models of

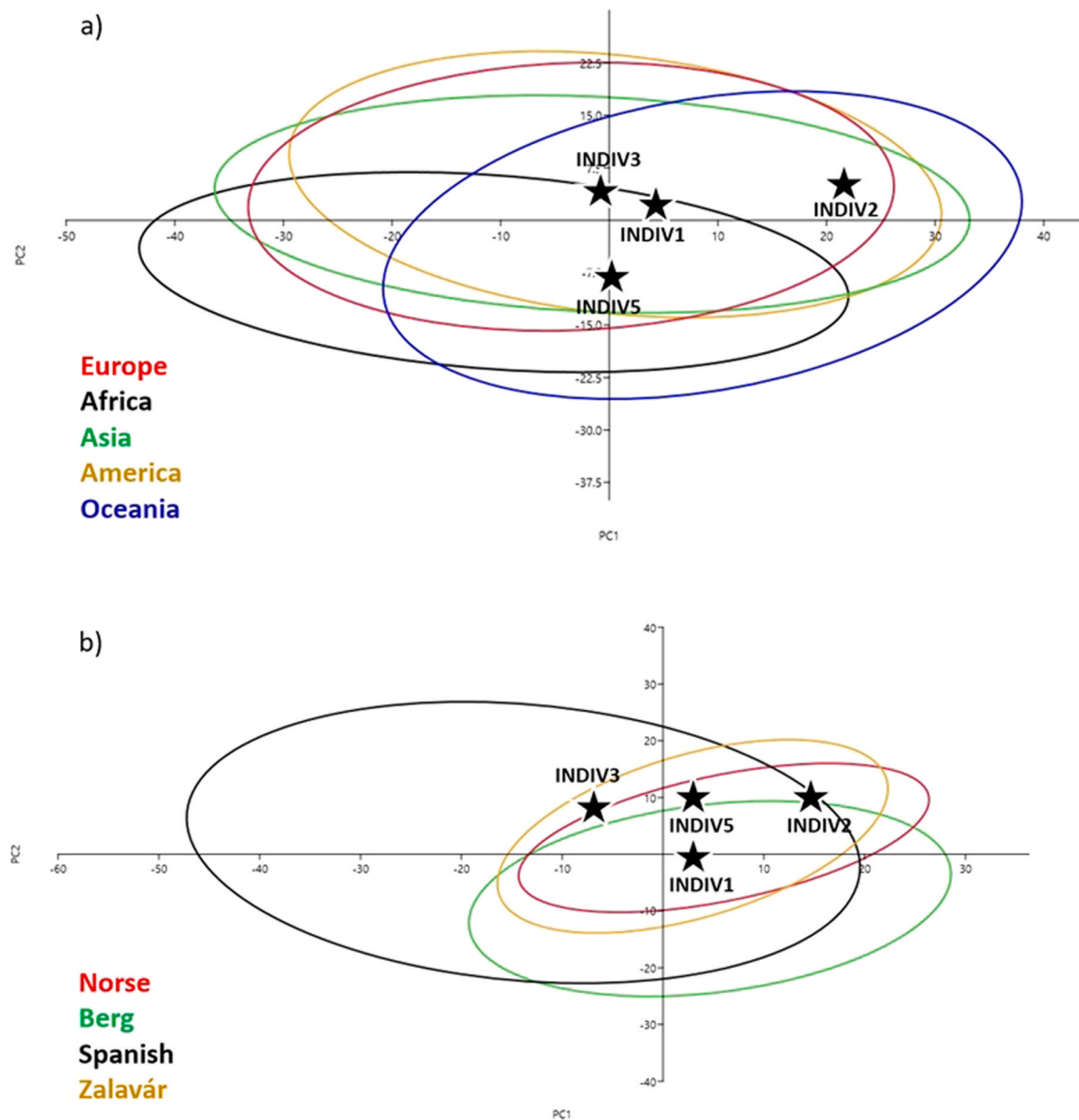


Fig. 8. Principal Component Analysis of the reference databases. A) PCA plot of the complete database (Howells+Olóriz) with samples grouped into five continents, with the first two PCs explaining 55 % of total craniofacial variance. B) PCA plot of the European database including four European samples, with the first two PCs explaining 45 % of total morphological variance. Confidence ellipses represent 95 % of variance within each continent or population.

small objects can be achieved using photogrammetry protocols based on macro images, allowing the 3D reconstruction of objects with dimensions in the order of few cm and measuring details smaller than 1 mm [79]; and small fragments as fractured portions of teeth can be assembled using digital techniques [80]. However, although digitalization and assembly may be technically feasible, the virtual reconstruction of skulls from many small fragments may not be practical considering the time and computational resources required to scan each fragment. Moreover, our assembly protocol requires the presence of several common anatomical points along the fracture edges of the fragments, limiting the potential of the method when bone portions are too small and fracture edges are not well-preserved. More advanced and automated protocols, including geometric morphometric approaches [28], are needed to overcome these limitations and to allow the reconstruction of highly fragmented skulls resulting from severe blast and comminuted trauma.

Our results further demonstrated that virtual skull reconstructions can be reliably used for morphological profiling [81]. Virtual

and traditional measurements presented deviations below 1.5 mm, indicating that 3D models generated by photogrammetry reliably reflect the size and shape of the original bones [51]. An additional benefit of virtual models is that they allow taking measurements in fragmented remains that cannot be glued in the laboratory but can be virtually assembled, as for example in INDIV5 (Fig. 4). Cranio-metric measurements on virtual reconstructions also showed a reduced intra-technique variability as compared to traditional metrics. This is likely due the fragmented state of some cranial remains, which increases the difficulty of keeping the skull in the same position during different measurement sessions and explains the dispersion of measures in Bland-Altman plots (Fig. 7). Therefore, traditional measures should not be taken as a “gold-standard” because measuring fragmented non-glued skulls using calipers is technically challenging and can introduce substantial measurement bias [76].

Besides reconstruction and measurement, the virtual restoration of craniofacial remains by symmetrization of cranial fragments

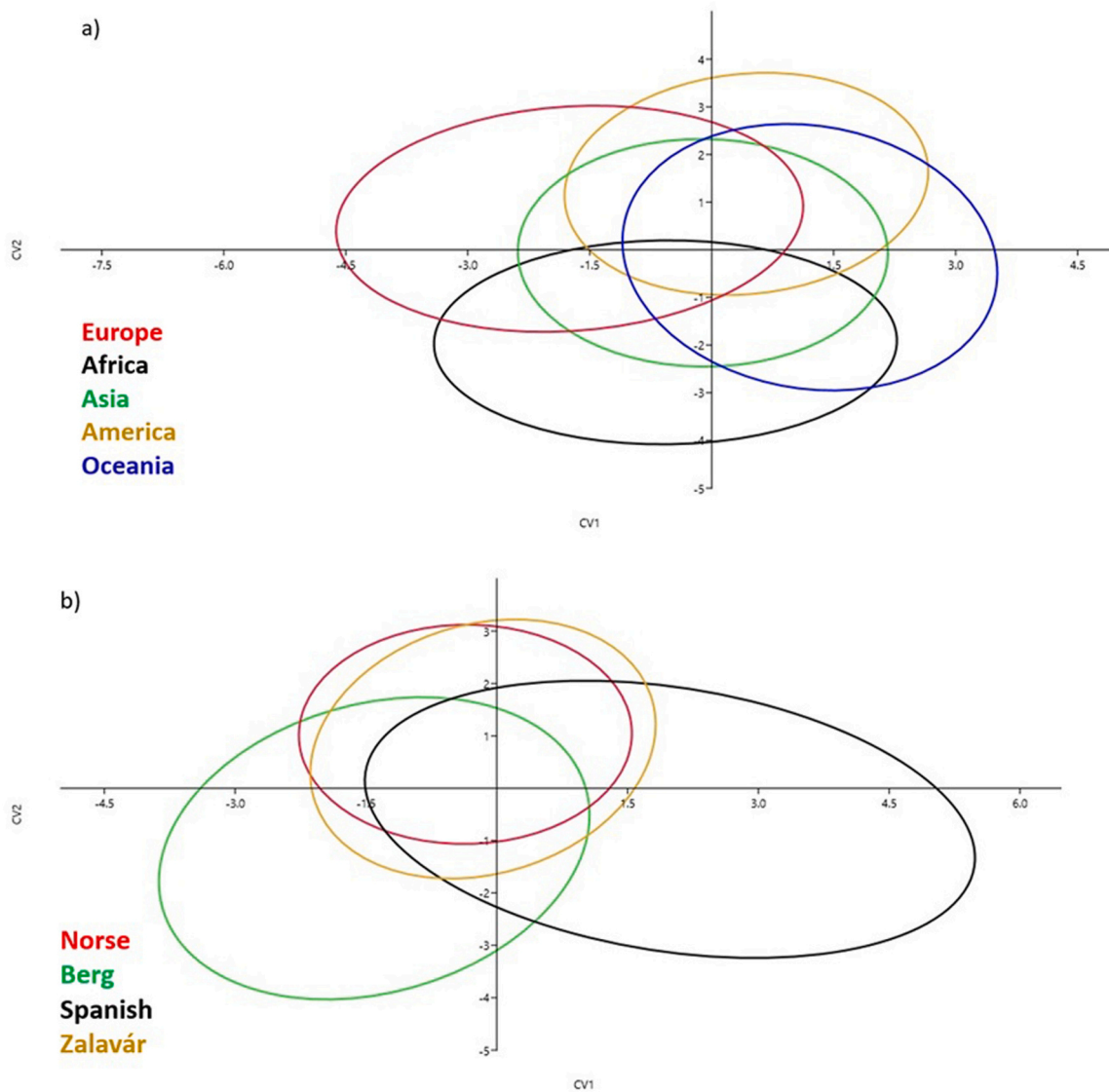


Fig. 9. Canonical Variate Analysis (CVA) of the reference databases. A) CVA plot of the complete database grouped into five continents. B) CVA plot of the European database including four European populations. Confidence ellipses represent 95 % of variance within each European population.

achieved the reduction of perimortem trauma and taphonomic postmortem modifications (Fig. 6). Although results were overall satisfactory, the method could be further improved by partial mirroring of the affected structures [82] and by applying geometric morphometrics to correct asymmetries and defects caused by trauma and taphonomic processes [83].

Finally, we explored the potential of restored virtual cranial reconstructions to test hypotheses of population ancestry and geographic origin [84]. Our results based on a sample of crania with known origin indicated that ancestry estimation was reliable for continental differentiation, achieving 86.7 % of correct classification, whereas correct Spanish ancestry estimation with high likelihood

was reduced to 27.3 % (Table 1). The overlap in cranial morphology observed in the morphospace created by the PCA and CVA analyses showed that variability across continents and countries is continuous and no clear-cut boundaries can be defined between populations based on cranial morphology (Figs. 8 and 9). Only craniofacial morphologies falling outside the continental or population overlap in the PCAs could be classified with high likelihood.

Results on the Spanish Civil War crania showed that, based on continental estimation, two out of four crania were classified as European and Asian with low posterior probabilities, suggesting that a non-European ancestry could be accepted. However, the range of craniofacial variation in Asia completely overlapped with the ranges

Table 2

Ancestry predictions in restored Spanish Civil War crania. Continental and European predictions associated to posterior probabilities. ¹ = all measurements included. ² = maximum cranial breadth not included. ³ = maximum cranial breadth and biauricular breadth not included.

Individual cranium	Continent prediction	Posterior probability	European prediction	Posterior probability
INDIV1 restored ¹	Europe	0.96	Norse	0.74
INDIV2 restored ¹	Europe	0.56	Spanish	0.86
INDIV3 restored ²	Asia	0.77	Spanish	0.95
INDIV5 restored ³	Africa	0.53	Spanish	0.52

of variation of the other continents (Figs. 8a and 9a), indicating a possible misclassification. At the European level, only two crania were estimated as Spanish with high associated posterior probabilities. Results from one cranium were not conclusive, and one cranium showed high similarity with the Norse sample, suggesting a non-Spanish population ancestry. However, these results were not endorsed by the archaeological evidence available. The robust individuals wearing gold dental caps and rings that were suspected as volunteers of the “International Brigade” of the Spanish Civil War (INDIV3 and INDIV5) were not estimated as non-Spanish European by the ancestry tests and further analyses are needed to confirm the hypothesis.

Our ancestry estimations based on cranial morphology are preliminary and could vary depending on the posterior probability threshold values considered (Table 2). High posterior probabilities (>0.9) indicate that an individual is morphologically very similar to the group classified, and therefore is likely more correctly classified than an individual classified with a low posterior probability (<0.7) [85]. Nevertheless, no cutoffs in posterior probabilities are required to correctly classify an unknown individual [86], and misclassifications can occur even with high posterior probabilities. Elliott & Collard (2009) suggested that an ancestry determination without ambiguity should have posterior probabilities higher than 0.991. Considering this conservative threshold, none of the classifications obtained in this study could be accepted without ambiguity.

To improve future analyses testing specific hypothesis about the geographical origin of cranial remains from the Spanish Civil War, the number of Spanish, European and world-wide samples used in the discriminant analyses should be increased, including larger samples of crania with known origin to further validate the method. When no reference populations of unknown crania are included in the analyses, misclassifications with other populations present in the sample may occur [43,87]. Moreover, to avoid biases induced by secular trends, which involve significant changes in the size and shape of the crania over time [88], cranial samples from contemporary populations should be favored over samples from different temporal periods, as for example the medieval Norse and Zalavár samples included in the Howells database [46]. Finally, 3D craniofacial models and geometric morphometrics analyses [48] could further enhance the potential of ancestry analysis.

In forensic research, the use of ancestry estimates is highly debated [89,90], and research should avoid typological approaches classifying individuals into social races based on craniometric traits [89,90]. These approaches have long been rejected and are not supported on scientific biological grounds [91,92]. However, the potential of craniofacial variation in biological anthropology studies can be leveraged following an evolutionary and population-based framework. Growing evidence supports that human craniofacial variation is genetically determined [93,94] and associated with population and sex differences [38,39,95], which leads to family resemblance and look-alike facial traits in unrelated individuals with genetic similarities [40,41,96,97]. As a result of complex evolutionary and population dynamics [98], genetic patterns surrogate population ancestry and these are reflected in phenotypic craniofacial differences among human populations [99].

In this context, approaches using craniometric traits to infer the geographical origin of unidentified individuals can help disentangle archeological issues. Considering the intrinsic limitations of population ancestry analyses [35,84], our results support that valuable information can be extracted from craniofacial remains for their biological profiling. Forensic cases like war victims are scenarios that need positive identification concerning their population of origin. Current methods grounded in statistical and population-specific analysis [90] can provide evidence to test archeological hypotheses, such as the presence of volunteers that served in the “International Brigade” in the Spanish Civil War.

5. Conclusions

Overall, our work demonstrates that the protocol for virtual reconstruction of cranial and mandibular remains using photogrammetric methods produced high quality results, as well as their virtual assembly and restoration. Virtual craniometry offered advantages in comparison to traditional methods, as additional measures could be taken on the skull remains and restored 3D models were less affected by fragmentation and deformation. Craniometric analysis showed that virtual 3D models can be used indistinctly from the actual remains for forensic applications. Current forensic use of ancestry estimation presents limitations, but our results indicate that craniofacial morphology has potential for ancestry assessment and can provide complementary information to other ancestry tests, especially when genetic testing is not available. Therefore, we recommend introducing virtual techniques in the biological and forensic anthropology disciplines when working with skeletal remains with perimortem trauma and taphonomic alterations, as in civil wars.

Funding

This research received funding from the Biological Anthropological Master of the Universitat Autònoma de Barcelona and the Universitat de Barcelona and from the Grup de Recerca Consolidat en Antropologia Biològica (GREAB, 2017 SGR 1630).

CRedit authorship contribution statement

Laia Sevillano Oriola: Conceptualization, Methodology, Formal analysis, Investigation, Data curation, Writing – original draft, Visualization. **Núria Armentano Oller:** Conceptualization, Validation, Resources, Writing – review & editing, Supervision, Project administration, Funding acquisition. **Neus Martínez-Abadías:** Conceptualization, Validation, Resources, Writing – review & editing, Supervision, Project administration, Funding acquisition.

Declaration of Competing Interest

The authors declare no competing interests.

Acknowledgements

We acknowledge the support of the Direcció General de Memòria Democràtica, Departament de Justícia de la Generalitat de Catalunya, for granting the access to study the skeletal material from the Spanish Civil War. We thank Max Rubert for continuous technical photographic assistance. Finally, we thank the reviewers and editor for constructive comments that have improved the quality of the manuscript.

Appendix A. Supporting information

Supplementary data associated with this article can be found in the online version at doi:10.1016/j.forsciint.2022.111504.

References

- [1] D. Ferembach, I. Schwidetzky, M. Stoukal, Recommendation for age and sex diagnoses of skeletons, *J. Hum. Evol.* 9 (1980) 517–549.
- [2] T. Todd, Age changes in the public bone; The white male pubis, *Am. J. Phys. Anthropol.* 3 (1920) 467–470.
- [3] C. Lovejoy, R. Meindl, T. Pryzbeck, R. Mensforth, Chronological metamorphosis of the auricular surface of the ilium – a new method for the determination of adult skeletal age at death, *Am. J. Phys. Anthropol.* 68 (1985) 15–28, <https://doi.org/10.1002/ajpa.1330680103>
- [4] M. Trotter, Estimation of stature from intact long bones, in: T.D. Stewart (Ed.), *Pers. Identif. Mass Disasters*, Smithsonian Institution, Washington DC, 1970.

- [5] J. Buikstra, D. Ubelaker, Standards for Data Collection from Human Skeletal Remains, *Ark. Archaeol. Surv. Res. Ser.* 44 (1994).
- [6] A. Castells Peig, Las Brigadas Internacionales en la Guerra de España, Ariel, Barcelona, 1974.
- [7] F. Etxeberria, Q. Solé, Fosas comunes de la Guerra Civil en el Siglo XXI: antecedentes, interdisciplinariedad y legislación, *Hist. Contemp.* 60 (2019) 401–438 (<http://hdl.handle.net/10810/38406>).
- [8] F. Serrulla Rech, Antropología forense de la Guerra Civil Española. Tesis doctoral, Universidad de Granada, 2018. (<http://hdl.handle.net/10481/54618>).
- [9] S. Palomo-Díez, C. Gomes, A.M. López-Parra, C. Baeza-Richer, I. Cuscó, C. Raffone, E. García-Arumí, D.C. Vinuesa-Espinosa, C. Santos, N. Montes, R. Rasal, O. Escala, J. Cuellar, E. Subirà, F. Casals, A. Malgosa, E. Tizzano, E. Tartera, G. Domenech, E. Arroyo-Pardo, Genetic identification of Spanish civil war victims. The state of the art in Catalonia (Northeastern Spain), *Forensic Sci. Int. Genet.* 7 (2019) 419–421, <https://doi.org/10.1016/j.fsigs.2019.10.035>
- [10] L. Ríos, J.L.C. Ovejero, J.P. Prieto, Identification process in mass graves from the Spanish Civil War I, *Forensic Sci. Int.* 199 (2010) e27–e36, <https://doi.org/10.1016/j.forsciint.2010.02.023>
- [11] J.M. Reverte Coma, Antropología forense, 2nd ed., Ministerio de Justicia. Secretaría General Técnica. Centro de Publicaciones, Madrid, 1999.
- [12] D. Gaudio, A. Betto, S. Vanin, A. De Guio, A. Galassi, C. Cattaneo, Excavation and study of skeletal remains from a World War I mass grave, *Int. J. Osteoarchaeol.* 25 (2015) 585–592, <https://doi.org/10.1002/oa.2333>
- [13] D.C. Kieser, R. Riddell, J.A. Kieser, J.-C. Theis, M.V. Swain, Bone micro-fracture observations from direct impact of slow velocity projectiles, *J. Arch. Mil. Med.* 2 (2014), <https://doi.org/10.5812/jamm.15614>
- [14] J.C. Love, J.M. Wiersema, Skeletal trauma: an anthropological review, *Acad. Forensic Pathol.* 6 (2016) 463–477, <https://doi.org/10.23907/2016.047>
- [15] P. Ribeiro, X. Jordana, S. Scheirs, M. Ortega-Sánchez, A. Rodríguez-Baeza, H. McGlynn, I. Galtés, Distinction between perimortem and postmortem fractures in human cranial bone, *Int. J. Leg. Med.* 134 (2020) 1765–1774, <https://doi.org/10.1007/s00414-020-02356-3>
- [16] D. Gaudio, L. De Luca, V. Cirielli, M. Caccianiga, C. Bassi, N. Cappelletto, A. Galassi, F. Nicolis, C. Cattaneo, Postmortem analysis of WWI human remains from Italian glaciers in rare environmental conditions, *Archaeol. Anthropol. Sci.* 11 (2019) 2569–2580, <https://doi.org/10.1007/s12520-018-0691-x>
- [17] R. Lyman, What taphonomy is, what it isn't, and why taphonomists should care about the difference, *J. Taphon.* 8 (2010) 1–16.
- [18] M.A. Pilloud, M.S. Megyesi, M. Truffer, D. Congram, The taphonomy of human remains in a glacial environment, *Forensic Sci. Int.* 261 (2016) 161.e1–161.e8, <https://doi.org/10.1016/j.forsciint.2016.01.027>
- [19] G. Grévin, P. Baillet, G. Quatrehomme, A. Ollier, Anatomical reconstruction of fragments of burned human bones: a necessary means for forensic identification, *Forensic Sci. Int.* 96 (1998) 129–134, [https://doi.org/10.1016/S0379-0738\(98\)00115-7](https://doi.org/10.1016/S0379-0738(98)00115-7)
- [20] B.G. Stephens, R. Heglar, Use of glue gun in forensic anthropology and pathologic bone reconstruction cases, *J. Forensic Sci.* 34 (1989) 12656J.
- [21] S. Benazzi, P. Bertelli, B. Lippi, E. Bedini, R. Caudana, G. Gruppioni, F. Mallegni, Virtual anthropology and forensic arts: the facial reconstruction of Ferrante Gonzaga, *J. Archaeol. Sci.* 37 (2010) 1572–1578, <https://doi.org/10.1016/j.jas.2010.01.018>
- [22] D. Fleming-Farrell, K. Michailidis, A. Karantanas, N. Roberts, E.F. Kranioti, Virtual assessment of perimortem and postmortem blunt force cranial trauma, *Forensic Sci. Int.* 229 (2013) 162.e1–162.e6, <https://doi.org/10.1016/j.forsciint.2013.03.032>
- [23] P. Urbanová, A.H. Ross, M. Jurda, I. Špíchalová, The virtual approach to the assessment of skeletal injuries in human skeletal remains of forensic importance, *J. Forensic Leg. Med.* 49 (2017) 59–75, <https://doi.org/10.1016/j.jflm.2017.05.015>
- [24] T. Uldin, Virtual anthropology – a brief review of the literature and history of computed tomography, *Forensic Sci. Res.* 2 (2017) 165–173, <https://doi.org/10.1080/20961790.2017.1369621>
- [25] A.J. Collings, K. Brown, Reconstruction and physical fit analysis of fragmented skeletal remains using 3D imaging and printing, *Forensic Sci. Int. Rep.* 2 (2020) 100114, <https://doi.org/10.1016/j.fsir.2020.100114>
- [26] G. Jani, A. Johnson, U. Parekh, T. Thompson, A. Pandey, Effective approaches to three-dimensional digital reconstruction of fragmented human skeletal remains using laser surface scanning, *Forensic Sci. Int. Synergy* 2 (2020) 215–223, <https://doi.org/10.1016/j.fsisy.2020.07.002>
- [27] G.W. Weber, Virtual anthropology, *Am. J. Phys. Anthropol.* 156 (2015) 22–42, <https://doi.org/10.1002/ajpa.22658>
- [28] P. Gunz, P. Mitteroecker, S. Neubauer, G.W. Weber, F.L. Bookstein, Principles for the virtual reconstruction of hominin crania, *J. Hum. Evol.* 57 (2009) 48–62, <https://doi.org/10.1016/j.jhevol.2009.04.004>
- [29] G.W. Weber, Another link between archaeology and anthropology: virtual anthropology, *Digit. Appl. Archaeol. Cult. Herit.* 1 (2014) 3–11, <https://doi.org/10.1016/j.daach.2013.04.001>
- [30] E. Bruner, B. Saracino, F. Ricci, M. Tafuri, P. Passarello, G. Manzi, Midsagittal cranial shape variation in the genus homo by geometric morphometrics, *Coll. Antropol.* 28 (2004) 99–112.
- [31] B. Musilová, J. Dupej, J. Bružek, Š. Bejdová, J. Velemínská, Sex and ancestry related differences between two Central European populations determined using exocranial meshes, *Forensic Sci. Int.* 297 (2019) 364–369, <https://doi.org/10.1016/j.forsciint.2019.02.034>
- [32] S. Grabherr, C. Cooper, S. Ulrich-Bochsler, T. Uldin, S. Ross, L. Oesterhelweg, S. Bolliger, A. Christophe, P. Schnyder, P. Mangin, M.J. Thali, Estimation of sex and age of “virtual skeletons”—a feasibility study, *Eur. Radiol.* 19 (2009) 419–429, <https://doi.org/10.1007/s00330-008-1155-y>
- [33] C. Villa, M.N. Hansen, J. Buckberry, C. Cattaneo, N. Lynnerup, Forensic age estimation based on the trabecular bone changes of the pelvic bone using post-mortem CT, *Forensic Sci. Int.* 233 (2013) 393–402, <https://doi.org/10.1016/j.forsciint.2013.10.020>
- [34] K.M. Spradley, R.L. Jantz, Ancestry estimation in forensic anthropology: geometric morphometric versus standard and nonstandard interlandmark distances, *J. Forensic Sci.* 61 (2016) 892–897, <https://doi.org/10.1111/1556-4029.13081>
- [35] E.F. Kranioti, J.G. García-Donas, I.O. Can, O. Ekizoglu, Ancestry estimation of three Mediterranean populations based on cranial metrics, *Forensic Sci. Int.* 286 (2018) 265.e1–265.e8, <https://doi.org/10.1016/j.forsciint.2018.02.014>
- [36] K. Harvati, T.D. Weaver, Human cranial anatomy and the differential preservation of population history and climate signatures, *Anat. Rec. Part A Discov. Mol. Cell. Evol. Biol.* 288A (2006) 1225–1233, <https://doi.org/10.1002/ar.a.20395>
- [37] W. Krogman, M. Iscan, *The Human Skeleton in Forensic Medicine*, Springfield, 1986.
- [38] J.H. Relethford, Craniometric variation among modern human populations, *Am. J. Phys. Anthropol.* 95 (1994) 53–62, <https://doi.org/10.1002/ajpa.1330950105>
- [39] C.C. Roseman, Detecting interregionally diversifying natural selection on modern human cranial form by using matched molecular and morphometric data, *Proc. Natl. Acad. Sci. U.S.A.* 101 (2004) 12824–12829, <https://doi.org/10.1073/pnas.0402637101>
- [40] E.A. Carson, Maximum likelihood estimation of human craniometric heritabilities, *Am. J. Phys. Anthropol.* 131 (2006) 169–180, <https://doi.org/10.1002/ajpa.20424>
- [41] N. Martínez-Abadías, M. Esparza, T. Sjøvold, R. González-José, M. Santos, M. Hernández, Heritability of human cranial dimensions: comparing the evolvability of different cranial regions, *J. Anat.* 214 (2009) 19–35, <https://doi.org/10.1111/j.1469-7580.2008.01015.x>
- [42] R. González-José, S. Van Der Molen, E. González-Pérez, M. Hernández, Patterns of phenotypic covariation and correlation in modern humans as viewed from morphological integration, *Am. J. Phys. Anthropol.* 123 (2004) 69–77, <https://doi.org/10.1002/ajpa.10302>
- [43] E. Cunha, D.H. Ubelaker, Evaluation of ancestry from human skeletal remains: a concise review, *Forensic Sci. Res.* 5 (2020) 89–97, <https://doi.org/10.1080/20961790.2019.1697060>
- [44] S. Ousley, R. Jantz, Fordisc 3: third generation of computer-aided forensic anthropology, *Rechtsmedizin* 23 (2013) 97–99, <https://doi.org/10.1007/s00194-013-0874-9>
- [45] D. Navega, C. Coelho, R. Vicente, M.T. Ferreira, S. Wasterlain, E. Cunha, AncestryTrees: ancestry estimation with randomized decision trees, *Int. J. Leg. Med.* 129 (2015) 1145–1153, <https://doi.org/10.1007/s00414-014-1050-9>
- [46] W.W. Howells, Cranial variation in man: A study by multivariate analysis of patterns of difference among recent human populations., Peabody Museum of American Archaeology and Ethnology, Harvard University, Cambridge (Mass.), 1973.
- [47] C. Maier, Evaluating mixed-methods models for the estimation of ancestry from skeletal remains, *Forensic Anthropol.* 2 (2019) 22–28, <https://doi.org/10.5744/fa.2018.1032>
- [48] D.E. Slice, A. Ross, 3D-ID: geometric morphometric classification of crania for forensic scientists., <http://www.3d-id.org>. (2009). (<https://www.3d-id.org/resources>).
- [49] D. Katz, M. Friess, Technical note: 3D from standard digital photography of human crania – a preliminary assessment, *Am. J. Phys. Anthropol.* 154 (2014) 152–158, <https://doi.org/10.1002/ajpa.22468>
- [50] H.M. Garvin, M.K. Stock, The utility of advanced imaging in forensic anthropology, *Acad. Forensic Pathol.* 6 (2016) 499–516, <https://doi.org/10.23907/2016.050>
- [51] B. Morgan, A.L.J. Ford, M.J. Smith, Standard methods for creating digital skeletal models using structure-from-motion photogrammetry, *Am. J. Phys. Anthropol.* 169 (2019) 152–160, <https://doi.org/10.1002/ajpa.23803>
- [52] Agisoft Metashape Standard, (2020).
- [53] C. Moraes, L. Bezzi, A. Bezzi, J. Šindelář, E. da Rosa, R. Dornelles, Modelo 3D vs fotogrametria por imagens e vídeo, *Figshare* (2022), <https://doi.org/10.6084/m9.figshare.20633262.v1>
- [54] N. Armentano, I. Galtés, Punta Sacarenyo PF0047. Estudi antropològic i forense, (2020).
- [55] N. Armentano, I. Galtés, E. Medina, M.E. Subirà, Fosses del carrer Ràfols (Sarrià, Barcelona). Estudi antropològic i forense, (2020).
- [56] R. Martin, K. Saller, *Lehrbuch der Anthropologie*, Stuttgart, 1957.
- [57] G. Olivier, *Pratique Anthropologique*, Paris, 1960.
- [58] C.N. Stephan, E.K. Simpson, Facial soft tissue depths in craniofacial identification (Part II): an analytical review of the published sub-adult data, *J. Forensic Sci.* 53 (2008) 1273–1279, <https://doi.org/10.1111/j.1556-4029.2008.00853.x>
- [59] T.D. White, M.T. Black, P.A. Folkens, *Human osteology: Third edition*, Hum. Osteol. Third Ed. (2011) 1–662.
- [60] A. Fedorov, R. Beichel, J. Kalpathy-Cramer, J. Finet, J.C. Fillion-Robin, S. Pujol, C. Bauer, D. Jennings, F. Fennessy, M. Sonka, J. Buatti, S. Aylward, J.V. Miller, S. Pieper, R. Kikinis, 3D Slicer as an image computing platform for the quantitative imaging network, *Magn. Reson. Imaging* 30 (2012) 1323–1341, <https://doi.org/10.1016/j.mri.2012.05.001>
- [61] E.F. Harris, R.N. Smith, Accounting for measurement error: a critical but often overlooked process, *Arch. Oral Biol.* 54 (2009) S107–S117, <https://doi.org/10.1016/j.archoralbio.2008.04.010>

- [62] K.E. Stull, M.L. Tise, Z. Ali, D.R. Fowler, Accuracy and reliability of measurements obtained from computed tomography 3D volume rendered images, *Forensic Sci. Int.* 238 (2014) 133–140, <https://doi.org/10.1016/j.forsciint.2014.03.005>
- [63] K. Aldridge, S.A. Boyadjiev, G.T. Capone, V.B. DeLeon, J.T. Richtsmeier, Precision and error of three-dimensional phenotypic measures acquired from 3dMD photogrammetric images, *Am. J. Med. Genet. Part A* 138A (2005) 247–253, <https://doi.org/10.1002/ajmg.a.30959>
- [64] R. Core Team, R: A language and environment for statistical computing., (2021).
- [65] B. Lehmert, BlandAltmanLeh: Plots (Slightly Extended) Bland-Altman Plots., (2015).
- [66] J.M. Bland, D.G. Altman, *Statistical methods for assessing agreement between two methods of clinical measurement*, *Lancet* 327 (1986) 307–310.
- [67] W.-C. Chiu Chiu, Estudio antropológico de la colección de cráneos Federico Olóriz, Universidad Complutense de Madrid, 2016.
- [68] F. Oloriz, Distribution de l'indice céphalométrique en Espagne, *Bull. Mem. Soc. Anthropol. Paris* 5 (1894) 520–525, <https://doi.org/10.3406/BMSAP.1894.5542>
- [69] N. Martínez-Abadías, R. González-José, A. González-Martín, S. Van der Molen, A. Talavera, P. Hernández, M. Hernández, Phenotypic evolution of human craniofacial morphology after admixture: a geometric morphometrics approach, *Am. J. Phys. Anthr.* 129 (2006) 387–398, <https://doi.org/10.1002/ajpa.20291>
- [70] L.W. Konigsberg, B.F.B. Algee-Hewitt, D.W. Steadman, Estimation and evidence in forensic anthropology: sex and race, *Am. J. Phys. Anthr.* 139 (2009) 77–90, <https://doi.org/10.1002/ajpa.20934>
- [71] R.L. Jantz, D.W. Owsley, Variation among early North American Crania, *Am. J. Phys. Anthropol.* 114 (2001) 146–155, [https://doi.org/10.1002/1096-8644\(200102\)114:2<146::AID-AJPA1014>3.0.CO;2-E](https://doi.org/10.1002/1096-8644(200102)114:2<146::AID-AJPA1014>3.0.CO;2-E)
- [72] D.A.T. Hammer, P.D. Ryan, Ø. Hammer, D.A.T. Harper, Past: paleontological statistics software package for education and data analysis, *Palaeontol. Electron.* 4 (2001) 178 (http://palaeo-electronica.org/2001_1/past/issue1_01.htm).
- [73] W.N. Venables, B.D. Ripley, *Modern Applied Statistics with S*, Fourth Edition, Springer, New York, 2002.
- [74] N. Armentano, J. Cuellar, I. Galtés, E. Gassiot, X. Jordana, C. Lalueza, M. Luna, A. Mahgosa, Q. Solé, M. Subirana, Informe sobre l'actuació a la Fossa de Gurb, Osona, 2009.
- [75] F. Alidoost, H. Arefi, Comparison of uas-based photogrammetry software for 3d point cloud generation: a survey over a historical site, *ISPRS Ann. Photogramm. Remote Sens. Spat. Inf. Sci.* (2017) 55–61, <https://doi.org/10.5194/isprs-annals-IV-4-W4-55-2017>
- [76] P. Urbanová, P. Hejna, M. Jurda, Testing photogrammetry-based techniques for three-dimensional surface documentation in forensic pathology, *Forensic Sci. Int.* 250 (2015) 77–86, <https://doi.org/10.1016/j.forsciint.2015.03.005>
- [77] G. Lauria, L. Sineo, S. Ficarra, A detailed method for creating digital 3D models of human crania: an example of close-range photogrammetry based on the use of Structure-from-Motion (SfM) in virtual anthropology, *Archaeol. Anthropol. Sci.* 14 (2022) 42, <https://doi.org/10.1007/s12520-022-01502-9>
- [78] S. White, C. Hirst, S.E. Smith, The suitability of 3D data: 3D digitisation of human remains, *Archaeologies* 14 (2018) 250–271, <https://doi.org/10.1007/s11759-018-9347-9>
- [79] A. Gallo, M. Muzzupappa, F. Bruno, 3D reconstruction of small sized objects from a sequence of multi-focused images, *J. Cult. Herit.* 15 (2014) 173–182, <https://doi.org/10.1016/j.culher.2013.04.009>
- [80] A. Johnson, G. Jani, J.A. Garriga, A. Pandey, Digital reconstruction of fragmented tooth remains in forensic context, *Forensic Sci. Res.* 7 (2022) 88–93, <https://doi.org/10.1080/20961790.2020.1737462>
- [81] R. Omari, C. Hunt, J. Coumbaros, B. Chapman, Virtual anthropology? Reliability of three-dimensional photogrammetry as a forensic anthropology measurement and documentation technique, *Int. J. Leg. Med.* 135 (2021) 939–950, <https://doi.org/10.1007/s00414-020-02473-Z/FIGURES/3>
- [82] K. Harvati, M. Leakey, J.-J. Hublin, C.C. Bauer, A virtual reconstruction and comparative analysis of the KNM-ER 42700 cranium, *Anthropol. Anz.* 72 (2015) 129–140, <https://doi.org/10.1127/anthranz/2015/0387>
- [83] A. Profico, L. Bellucci, C. Buzi, F. Di Vincenzo, I. Micarelli, F. Strani, M.A. Tafuri, G. Manzi, Virtual anthropology and its application in cultural heritage studies, *Stud. Conserv.* 64 (2018) 323–336, <https://doi.org/10.1080/00393630.2018.1507705>
- [84] R.R. Dunn, M.C. Spiros, K.R. Kamnikar, A.M. Plemons, J.T. Hefner, Ancestry estimation in forensic anthropology: a review, *WIREs Forensic Sci.* 2 (2020), <https://doi.org/10.1002/WFS2.1369>
- [85] R.L. Jantz S.D. Ousley *FORDISC*, Version 3 2005 0.
- [86] S.D. Ousley, R.L. Jantz, *Fordisc 3 and statistical methods for estimating sex and ancestry*, in: D. Dirkmaat (Ed.), *A Companion to Forensic Anthropol*, Blackwell Publishing Ltd, 2012, pp. 311–329.
- [87] M. Elliott, M. Collard, *FORDISC* and the determination of ancestry from cranial measurements, *Biol. Lett.* 5 (2009) 849–852, <https://doi.org/10.1098/rsbl.2009.0462>
- [88] R.L. Jantz, L. Meadows Jantz, Secular change in craniofacial morphology, *Am. J. Hum. Biol.* 12 (2000) 327–338, [https://doi.org/10.1002/\(SICI\)1520-6300\(200005/06\)12:3<327::AID-AJHB3>3.0.CO;2-1](https://doi.org/10.1002/(SICI)1520-6300(200005/06)12:3<327::AID-AJHB3>3.0.CO;2-1)
- [89] J.D. Bethard, E.A. DiGangi, Moving beyond a lost cause: forensic anthropology and ancestry estimates in the United States, *J. Forensic Sci.* 65 (2020) 1791–1792, <https://doi.org/10.1111/1556-4029.14513>
- [90] K.E. Stull, E.J. Bartelink, A.R. Klales, G.E. Berg, M.W. Kenyhercz, E.N. L'Abbé, M.C. Go, K. McCormick, C. Mariscal, Moving beyond a lost cause: Forensic anthropology and ancestry estimates in the United States, *J. Forensic Sci.* (2021) 417–420, <https://doi.org/10.1111/1556-4029.14616>
- [91] J.M. Organ, A.R. Comer, Evolution of a discipline—The changing face of anatomy, *Anat. Rec.* (2022) 766–771, <https://doi.org/10.1002/ar.24901>
- [92] J.A. Raff, C.J. Mulligan, Race reconciled < scp > II < /scp > :interpreting and communicating biological variation and race in 2021, *Am. J. Phys. Anthropol.* 175 (2021) 313–315, <https://doi.org/10.1002/ajpa.24291>
- [93] J. Roosenboom, G. Hens, B.C. Mattern, M.D. Shriver, P. Claes, Exploring the underlying genetics of craniofacial morphology through various sources of knowledge, *Biomed. Res. Int.* (2016) (2016), <https://doi.org/10.1155/2016/3054578>
- [94] S. Richmond, L.J. Howe, S. Lewis, E. Stergiakouli, A. Zhurov, Facial genetics: a brief overview, *Front. Genet.* 9 (2018) 462, <https://doi.org/10.3389/FGENE.2018.00462/XML/NLM>
- [95] J.H. Relethford, Race and global patterns of phenotypic variation, *Am. J. Phys. Anthr.* 139 (2009) 16–22, <https://doi.org/10.1002/AJPA.20900>
- [96] N. Martínez-Abadías, M. Esparza, T. Sjøvold, R. González-José, M. Santos, M. Hernández, C.P. Klingenberg, Pervasive genetic integration directs the evolution of human skull shape, *Evolution* 66 (2012) 1010–1023, <https://doi.org/10.1111/j.1558-5646.2011.01496.x>
- [97] R.S. Joshi, M. Rigau, C.A. García-Prieto, M. Castro de Moura, D. Piñeyro, S. Moran, V. Davalos, P. Carrión, M. Ferrando-Bernal, I. Olalde, C. Lalueza-Fox, A. Navarro, C. Fernández-Tena, D. Aspandi, F.M. Sukno, X. Binefa, A. Valencia, M. Esteller, Look-alike humans identified by facial recognition algorithms show genetic similarities, *Cell Rep.* 40 (2022) 111257, <https://doi.org/10.1016/j.CELREP.2022.111257/ATTACHMENT/C26B1508-DECB-4B2F-85AA-540B17ECE362/MMC8.XLSX>
- [98] L. Qiao, Y. Yang, P. Fu, S. Hu, H. Zhou, S. Peng, J. Tan, Y. Lu, H. Lou, D. Lu, S. Wu, J. Guo, L. Jin, Y. Guan, S. Wang, S. Xu, K. Tang, Genome-wide variants of Eurasian facial shape differentiation and a prospective model of DNA based face prediction, *J. Genet. Genom.* 45 (2018) 419–432, <https://doi.org/10.1016/j.JGG.2018.07.009>
- [99] M. Quinto-Sánchez, K. Adhikari, V. Acuña-Alonso, C. Cintas, C.C. Silva de Cerqueira, V. Ramallo, L. Castillo, A. Farrera, C. Jaramillo, W. Arias, M. Fuentes, P. Everardo, F. de Avila, J. Gomez-Valdés, T. Hünemeier, S. Gibbon, C. Gallo, G. Poletti, J. Rosique, M.C. Bortolini, S. Canizales-Quinteros, F. Rothhammer, G. Bedoya, A. Ruiz-Linares, R. González-José, Facial asymmetry and genetic ancestry in Latin American admixed populations, *Am. J. Phys. Anthropol.* 157 (2015) 58–70, <https://doi.org/10.1002/ajpa.22688>